

Original Article

*Both authors contributed equally to the work.

Cite this article: Martin-Cao-Romero C, Solís-Marín FA, Bribiesca-Contreras G (2021). *Crinitostella laguardai*, new genus and species of wood-dwelling deep-sea sea-star (Asteroidea: Caymanostellidae) from the Gulf of Mexico. *Journal of the Marine Biological Association of the United Kingdom* **101**, 591–597. <https://doi.org/10.1017/S0025315421000448>

Received: 9 February 2021

Revised: 11 May 2021

Accepted: 2 June 2021

First published online: 30 June 2021

Key words:


Asteroidea; Caymanostellidae; deep-sea; Gulf of Mexico; Valvatida; Velatida; wood-dwelling

Author for correspondence:

Guadalupe Bribiesca-Contreras,

E-mail: l.bribiesca-contreras@nhm.ac.uk

Crinitostella laguardai, new genus and species of wood-dwelling deep-sea sea-star (Asteroidea: Caymanostellidae) from the Gulf of Mexico

Carolina Martin-Cao-Romero^{1,*}, Francisco Alonso Solís-Marín²
and Guadalupe Bribiesca-Contreras^{3,*} 

¹Posgrado en Ciencias del Mar y Limnología, Universidad Nacional Autónoma de México, Mexico City, Mexico;

²Laboratorio de Sistemática y Ecología de Equinodermos, Colección Nacional de Equinodermos “Dra. Ma. E. Caso Muñoz”, Instituto de Ciencias del Mar y Limnología, Universidad Nacional Autónoma de México, Circuito Universitario s/n, Mexico City, 04510, Mexico and ³Natural History Museum, London, UK

Abstract

The Caymanostellidae is a family of rarely encountered wood-dwelling deep-sea sea-stars, with only six species, in two genera, described to date. During the COBERPES 5 expedition on board the RV ‘Justo Sierra’, off Tabasco, Gulf of Mexico in 2013, 12 specimens were recovered from a single piece of sunken wood. Herein we describe a new genus and species of caymanostellid, *Crinitostella laguardai* gen. nov., sp. nov. This species represents the shallowest known caymanostellid (418–427 m depth), and the first known occurrence of the Caymanostellidae from the Gulf of Mexico. The family Caymanostellidae displays affinities with several groups, such as Asterinidae and Korethrasteridae, making it difficult to infer its phylogenetic position evidenced by the myriad of contrasting phylogenetic hypotheses proposed. In an attempt to shed some light on the phylogenetic relationships of the family, sequences of nuclear and mitochondrial DNA of the new species were generated and combined with published data. As previously suggested, caymanostellids seem to be part of valvatcean polytomy rather than velatids.

Introduction

The family Caymanostellidae Belyaev, 1974 includes sea-stars that are associated with deep-sea wood substrates in lower bathyal to abyssal depths. Representatives of the family have been found in the Indian, Atlantic and Pacific Oceans, with only six species in two genera described to date (Mah & Blake, 2012; Mah, 2019). The family was first established by Belyaev (1974), who considered it to be a member of the order Phanerozoia. Then, based on the resemblance of abactinal and marginal plates to those of members of the family Asterinidae, it was placed within the order Spinulosida (Aziz & Jangoux, 1984). After that, caymanostellids were considered aberrant velatidans, more closely related to the family Korethrasteridae, and the order Velatida was re-established to include these two families along with Solasteridae, Myxasteridae and Pterasteridae (Blake, 1987). Smith (1988) agreed with this ordinal position, and proposed a subgroup including the Caymanostellidae and Xyloplacidae, as both families include wood-dwelling deep-sea species. However, Rowe *et al.* (1988) suggested Asterinidae, Korethrasteridae and Caymanostellidae to share a valvatid-type ancestor, and retained them within Valvatida. More recently, molecular studies showed that Pterasteridae and Xyloplacidae are not closely related to either Caymanostellidae or Pterasteridae, with Caymanostellidae not recovered within Velatida, but its phylogenetic position was uncertain (Janies *et al.*, 2011). Additionally, a morphological review of asteroids has suggested the family to form part of a valvatcean polytomy (Mah & Blake, 2012). Despite this, the family is still formally included in the order Velatida (McKnight, 2006; Mah, 2019).

The genus *Caymanostella* Belyaev, 1974 was the first to be described and it currently includes four species: *C. admiranda* Belyaev & Litvinova, 1977, collected from the Coral Sea (5220 m); *C. madagascarensis* Belyaev & Litvinova, 1991, collected from off the west coast of Madagascar (1500 m); *C. phorcynis* Rowe, 1989, collected from the Tasman Sea (736–1208 m); and *C. spinimarginata* Belyaev, 1974, collected from the Cayman Trench (6740–6780 m). The genus *Belyaevostella* Rowe, 1989 was described after an extensive revision of caymanostellids and it includes two species: *B. hispida* (Aziz & Jangoux, 1984), collected from the Macassar Straits (1301–2350 m); and *B. hyugaensis* Fujita, Stapanato & Jangoux 1994, collected from the Hyuga Basin (1650 m).

This paper describes a new genus and species of caymanostellid that was collected during the oceanographic survey COBERPES 5 on board the RV ‘Justo Sierra’, in the Gulf of Mexico. Specimens were associated with sunken wood, as are other species in this family. The set of morphological characters differs from those described for both existing genera, supporting the erection of a new genus. In addition, we obtained genetic sequences for the new genus/species



to provide some insight into the phylogenetic relationships of the family Caymanostellidae, and suggest its placement within the order Valvatida.

Materials and methods

Sampling

During the scientific expedition COBERPES 5, on board the RV 'Justo Sierra', a log was recovered from a trawl (see Ramirez *et al.*, 2019, for details on sampling method) at 418–427 m depth, off Tabasco, in the Gulf of Mexico. Once on deck, the piece of wood was broken apart and carefully inspected for any wood-associated fauna. Twelve caymanostellid specimens were recovered and immediately preserved in 70% non-denatured ethanol. Specimens were shipped to the Instituto de Ciencias del Mar y Limnología, Universidad Nacional Autónoma de México, Mexico, for further analysis.

Morphological examination

A detailed morphological examination of the specimens collected was carried out. In addition, comparative material from other species within the genera *Caymanostella* and *Balyaevostella* was examined. The holotype (ICML-UNAM 18415) was photographed using a multifocal microscope (Olympus SZX12-MDU). In addition, one paratype (ICML-UNAM 18416) was mounted on an aluminium stub and gold-coated for scanning electron microscopy (SEM; Hitachi SU1510, Instituto de Biología, Universidad Nacional Autónoma de México) analysis. SEM analysis was also performed after the skin, actinal, and abactinal armament were removed using undiluted bleach. Additional photographs were taken from another paratype (NHMUK 2021.2), using a Canon 5D Mark II camera and stacked using the Zerene Stacker software at Museums Victoria, Melbourne, Australia before and after exposure to undiluted bleach.

DNA extraction, amplification, and sequencing

Tube feet from another specimen (NHMUK 2021.1) were used for genetic analyses. DNA extraction was performed using the DNeasy Blood and Tissue Kit (Qiagen). We targeted several genes, but we were able to successfully amplify 16S and the early-stage histone H3 gene. Each PCR reaction contained 10.5 µl of Red Taq DNA Polymerase 1.1× MasterMix (VWR), 0.5 µl of each primer (10 µM), and 1 µl of DNA template. The 16S gene was amplified using the primers 16sar-L (CGCCTGTTTATCAAAAACAT) and 16sbr-H (CCGGTCTGAACTCAGATCACGT) (Palumbi, 1996), and H3 with H3F (ATGGCTCGTACCAAGCAGACVGC) and H3R (ATATCCTTRGGCATRATRGTGAC) (Colgan *et al.*, 2003). Both fragments were amplified using an initial denaturation at 94°C for 2 min, followed by 30 cycles of denaturation at 94°C for 15 s, annealing at 55°C for 30 s, extension at 68°C for 30 s, and a final extension at 68°C for 4 min. PCR products were purified and sequenced, using the same primers as for amplification, at The Natural History Museum Sequencing Facilities using a Millipore Multiscreen 96-well PCR Purification System and ABI 3730XL DNA Analyser (Applied Biosystems), respectively. Contigs were assembled from both forward and reverse sequences using Geneious 7.0.6 (<https://www.geneious.com>) and chromatograms were visually inspected for ambiguous base calls, which were corrected manually. Generated sequences for the H3 and 16S genes were deposited in GenBank with accession numbers MW556265 and MW556266, respectively.

Phylogenetic analyses

In order to provide some insight into the phylogenetic relationships of the family we estimated a phylogenetic tree. In addition to the sequences for the 16S and H3 genes generated for this study, we included sequences from public databases for the 12S, 16S, 18S, 28S, H3, and COI genes (Supplementary S1). Protein-coding genes (COI and H3) were aligned using MUSCLE in MEGA X (Kumar *et al.*, 2018), and nucleotides translated into amino acids to identify pseudogenes by the presence of stop codons. Non protein-coding genes (12S, 16S, 18S and 28S) were aligned using MAFFT version 7 (Katoh *et al.*, 2019) using the auto strategy, and unalignable regions filtered in GBLOCKS (Castresana, 2000) allowing gap positions within final blocks and less strict flanking positions. Individual gene-alignments were concatenated in Geneious 7.0.6 (<https://www.geneious.com>), and the best substitution model for each partition (each gene and each codon position for protein-coding genes) was determined using PartitionFinder (Lanfear *et al.*, 2017).

Phylogenetic trees were estimated using partitioned maximum-likelihood (RAxML v8.2.10; Stamatakis, 2006) and Bayesian inference (BEAST v2.4.7; Bouckaert *et al.*, 2014) approaches, with the best inferred substitution model for each partition. The best ML tree and support values were estimated from 1000 rapid bootstrap and 20 ML searches using HKY85 substitution model for all partitions (Supplementary S2). BEAST analyses were performed with trees and clock models linked, a Yule tree model, and relaxed clock log normal. Two independent runs of a maximum 100 M steps were combined after discarding 20% as burn-in. Runs were checked for convergence and a median consensus tree was estimated from the combined post-burn-in samples (Supplementary S3). For both analyses, the orders were constrained based on results from phylogenomic methods (Linchangco *et al.*, 2017). Posterior probability and support values from both BI and ML analyses were summarized in the median BEAST tree.

List of institutional abbreviations

ICML-UNAM: Colección Nacional de Equinodermos 'Dra. Ma. Elena Caso Muñoz', Instituto de Ciencias del Mar y Limnología, Universidad Nacional Autónoma de México, México; MV: Museums Victoria, Melbourne, Australia; NHMUK: Natural History Museum, London; NSMT: National Museum of Natural and Science, Tokyo, Japan.

Results

Systematics

Order VALVATIDA Perrier, 1884
 Family CAYMANOSTELLIDAE Belyaev, 1974
 Genus *Crinitostella* gen. nov.
 LSID urn:lsid:zoobank.org:
 act:2A2AB767-2DFA-4D16-A93D-376B1C1E6B86

Type Species

Crinitostella laguardai gen. nov., sp. nov.

Other Species Included

None.

Etymology

From the latin word *crinitus*, which means hairy, referring to the fluffy or hairy appearance of the caymanostellid sea-star. Gender feminine.

Description

Caymanostellid sea star with stellate body, covered by a thin skin obscuring the outline of abactinal plates, except the proximal

carinal plates. Abactinal scalar plates, wider than long, thin, perforated and slightly imbricated. Carinal plates form a longitudinal row, with a row of dorsal-lateral plates on each side and the central disc plates arranged in irregular cycles. Supero- and infero-marginal plates similar in size; superomarginal plates subovate, longer than wide; inferomarginal plates subcircular, slightly longer than wide. Gonopores not visible. Simple madreporite, Y-shaped. Aboral papulae absent. Actinal membrane heart-shaped, with no embedded spicules. Adambulacral and oral plates as for family.

Remarks

Crinitostella gen. nov. is distinguished from *Caymanostella* in having a spiniform abactinal armament compared with the granular armament in the latter genus. It differs from *Belyaevostella* in lacking abactinal papulae and spicules on the actinal membrane, as well as having supero- and inferomarginal plates which are similar in size. *Crinitostella* gen. nov. differs from both genera in lacking conspicuous gonopores. It also differs from both existing genera in the shape and pattern of the abactinal plates, which are delicate as in *Belyaevostella*, but perforated and pentagonal to hexagonal in shape, with very rounded angles, being almost oval-shaped, longer than wide. Abactinal plates are arranged in two fields, more similar to *Caymanostella*, with the central disc plates imbricating regularly but arranged in somewhat irregular cycles until the distal lateral disc plates. Similar to *Caymanostella*, there is a well-defined longitudinal row of carinal plates that runs from the distal lateral disc plates to the tip of the arm, but with a single well-defined row, instead of two, of dorsal-lateral plates on each side.

Crinitostella laguardai gen. nov., sp. nov.

LSIDurn:lsid:zoobank.org:act:

F19DD701-5F8B-4313-B301-2279202EF0B8

(Figures 1 & 2)

Type Material

Holotype (ICML-UNAM 18415): adult specimen preserved dry $R = 3$ mm, $r = 2.25$ mm, (COBERPES 5, A15; coordinates: 19°16.272'N 93°06.69'W to 19°16.045'N 93°04.613'W; water depth: 418–427 m); coll. A. Caballero, J. Arriaga and M. Valdes, 25 May 2013.

Paratype (ICML-UNAM 18416): adult specimen preserved dry $R = 3.5$ mm, $r = 2.2$ mm, (COBERPES 5, A15; coordinates: 19°16.272'N 93°06.69'W to 19°16.045'N 93°04.613'W; water depth: 418–427 m); coll. A. Caballero, J. Arriaga and M. Valdes, 25 May 2013.

Paratype (NHMUK 2021.1): adult specimen preserved in 80% non-denatured ethanol $R = 3.2$ mm, $r = 2.3$ mm, (COBERPES 5, A15; coordinates: 19°16.272'N 93°06.69'W to 19°16.045'N 93°04.613'W; water depth: 418–427 m); coll. A. Caballero, J. Arriaga and M. Valdes, 25 May 2013; GenBank accession numbers MW556265 (H3) and MW556266 (16S).

Paratype (NHMUK 2021.2): adult specimen preserved in 80% non-denatured ethanol $R = 3.2$ mm, $r = 2.1$ mm, (COBERPES 5, A15; coordinates: 19°16.272'N 93°06.69'W to 19°16.045'N 93°04.613'W; water depth: 418–427 m); coll. A. Caballero, J. Arriaga and M. Valdes, 25 May 2013.

Eight additional specimens preserved in 70% non-denatured ethanol (ICML-UNAM 18417).

Comparative Material Examined

Belyaevostella hyugaensis Fujita, Stapanato & Jangoux, 1994. Holotype: one specimen preserved dry (NSMT-E 3001); Cruise KT-86-t6, Station D2 (Hyuga Basin, off southern Japan, western

North Pacific: 32°21.1'N 132°28.5'E to 32°19.1'N 132°28.6'E); collected on 2 November 1986, 1650–1653 m depth.

Caymanostella spinimarginata Belyaev, 1974. Paratype: one specimen preserved in ethanol (NHM 1987.3.26.2); RV 'Akad. Kurchatov', Station 1267 (Oriente depression, eastern part of Cayman Trench: 19°38.5'S 76°35'W); 6740–6780 m depth.

Caymanostella admiranda Belyaev & Litvinova, 1977. Paratype: one specimen preserved in ethanol (NHM 1987.3.26.3); RV 'Akad. Mendeleev', Station 1234 (Coral Sea: 7°31.1'S 149°51.1'E); 5220 m depth.

Etymology

Named in honour of Dr Alfredo Laguarda Figueras, who played a key role in the consolidation of marine sciences in Mexico. He has been a researcher for over 50 years, and for the last 30 years he has also been fundamental to the study of echinoderms in Mexico, acting as the keeper of Dr Maria Elena Caso's echinoderm legacy.

Diagnosis

Five rays, body form stellate. Rays broad at the base, rounded at ambitus. Thin, somewhat petaloid furrows. Skeletal plates are covered by a thin epidermis that obscures the base of the spinelets and the edges of the plates, except for proximal carinal plates. Abactinal plates ovate, wider than long, imbricated except for proximal carinal ones, where both proximal and distal edges are not covered. Supero- and inferomarginal plates of similar size (width), but supero- are longer than inferomarginal. Large, sub-rectangular terminal plate, which bears a single papula with a pore almost half the width of the plate in diameter. Abactinal spinelets numerous and irregularly distributed over abactinal plates, club-shaped, with longitudinal ridges, somewhat flat but with thorny tips. Spinelets on inferomarginal plates are not arranged forming a fringe along the ambitus; longer and thinner than the rest of abactinal spinelets, with base almost as wide as the tip; tip is somewhat rounded and thorny. Actinal plates absent. Bar-like ambulacral plates extend from the ambulacral furrow to the abactinal openings. Each ambulacral plate bears 2–4, mostly 2, furrow spines, and several numerous actinal spinelets arranged in irregular rows. Actinal spinelets are longer than spinelets on inferomarginal plates; slender, covered with small but stout thorns, base wider than the tip, tip is rounded. Each oral plate bears 5 oral spines arranged in 2 proximal, and 3 distal; and 3 (sometimes 4) suboral spines arranged in 1 (sometimes 2) proximal, 1 central, and 1 distal; similar in shape to actinal spinelets but somewhat curvate.

Holotype Description

Size: $R = 3$ mm, $r = 2.25$ mm (examined specimens range in size $R = 2.7$ – 3.9 mm, $r = 1.1$ – 2.9 mm). Five rays, body form stellate (Figures 1A, F & 2A, B). Rays broad at the base rounded at ambitus. Furrows are thin, but slightly petaloid (Figures 1B & 2B). Abactinal surface slightly convex, sunken at the interradii; actinal surface flat. There is a thin skin covering the abactinal surface, which obscures the limits of the plates on the interradii and the base of the spinelets. Abactinal skeleton composed of thin, perforated plates (only visible using SEM; Figure 2E, F; when observed using a stereoscopic microscope, plates appear to have glassy convexities), which are pentagonal to hexagonal, with rounded angles making them almost oval, wider than long. Abactinal plates are imbricated distally and arranged in two fields. The central disc plates are arranged in somewhat irregular cycles until the distal lateral disc plate (Figures 1G & 2E). Carinal plates are larger than the rest of the abactinal plates, ovate, less than two times as wide as long ($L = 190$ μ m, $W = 340$ μ m); forming a well-defined longitudinal row from the tip of the arm until about 2/3 R where the distal lateral disc plates are located; proximal carinal plates are not imbricated between them, so proximal and distal edges are

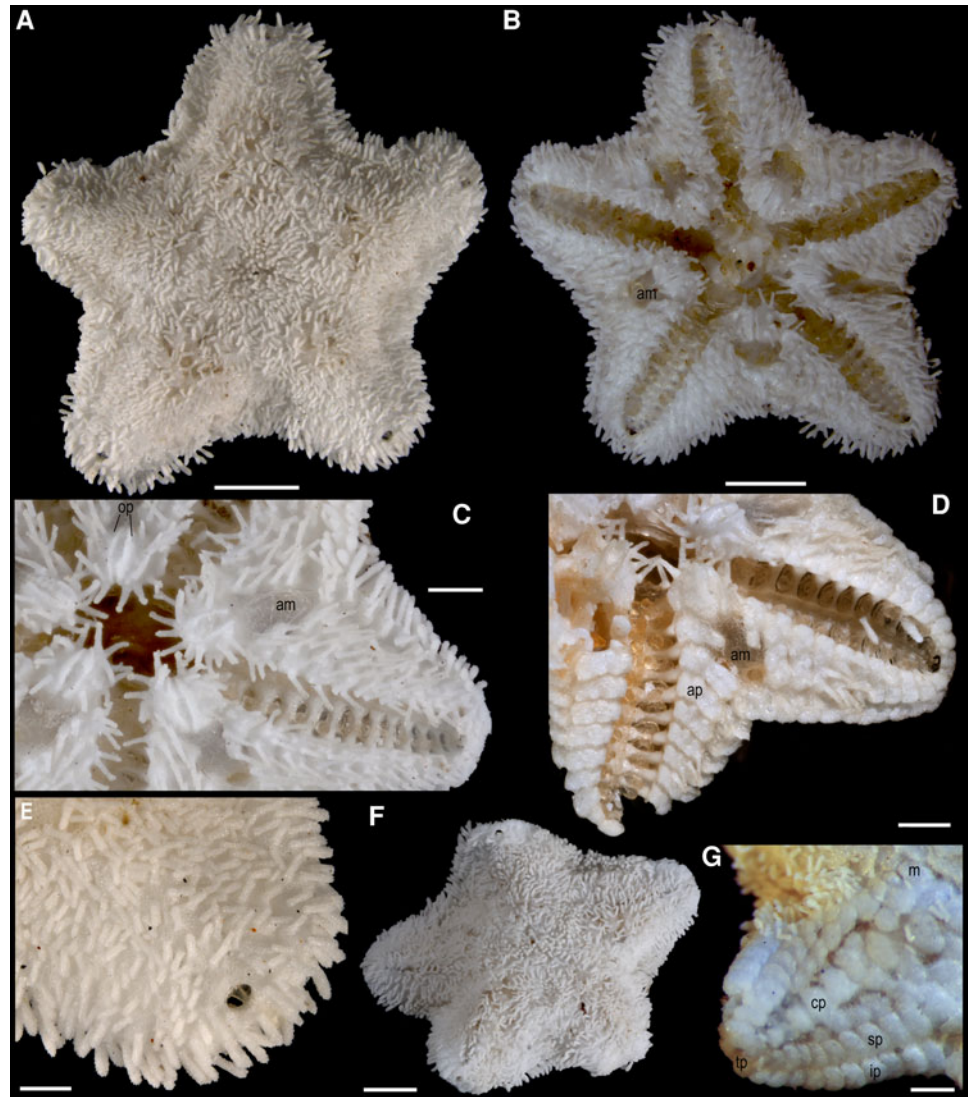


Fig. 1. *Crinitostella laguardai* gen. nov., sp. nov. Holotype (ICML-UNAM 18415): abactinal surface (A); actinal surface (B); details of actinal surface (C); tip of arm with pore and papula on terminal plate (E). Paratype (NHMUK 2021.2): detail of denuded actinal surface (D); abactinal surface (F); detail of denuded plates on abactinal surface (G). Scale bars: A, B, F, 1 mm; C, D, 500 μ m; E, G, 250 μ m. am, actinal membrane; op, oral plate; ap, ambulacral plate; cp, carinal plate; sp, superomarginal plate; ip, inferomarginal plate; tp, terminal plate; m, madreporite.

not obscured by other plates nor by the epidermis. There is a single longitudinal row of dorsal-lateral plates on each side of the carinal row. Each ray possesses a large terminal plate ($\sim 400 \mu$ m long and $\sim 340 \mu$ m wide), sub-rectangular, and perforated; bearing a large, single papula which diameter ($\sim 155 \mu$ m) equals almost half the width of the terminal plate (Figures 1E & 2F). Papillae absent on the abactinal surface. The madreporite is large, Y-shaped, obscured by abactinal spinelets (Figure 1G). The ambitus is defined by two rows of imbricated marginal plates. Supero- and inferomarginal plates similar in size (length); superomarginals are ovate, almost twice as long as wide (Figure 1G); proximal-most inferomarginal plate subcircular, slightly longer than wide, becoming smaller and longer towards the tip of the arm, with the distal-most being sub-triangular, still longer than wide. Abactinal spinelets are numerous and close together, especially on the proximal region of the disc, but more scattered on the carinal region (3–8 spines per plate); spinelets are $\sim 100 \mu$ m in length, club-shaped, porous, with 10 (mostly) longitudinal ridges, somewhat flat at the tip but with several small thorns, from which the ones at the centre of the tip are taller than the ones at the margin of the tips (Figure 2H). Superomarginal plates are also covered by spinelets like those on the adoral plates. Spinelets on inferomarginal plates are longer ($\sim 200 \mu$ m), more slender, with less defined longitudinal ridges, and more rounded tips than the abactinal spinelets, thorns appear both on the tips

and along the longitudinal ridges; the base is barely narrower than the tip; they are irregularly arranged, not forming a fringe along the ambitus (Figure 2G).

Actinal plates absent (Figure 1D). Bar-like ambulacral plates extend from the ambulacral furrow to the abactinal openings; wider than long and diagonally positioned with the ambulacral furrow; adradial side is rounded and abradial side is straight (Figure 1D). The first and last plates are triangular rather than bar-like. Ambulacral plates are less porous than abactinal ones. Actinal spines are longer ($\sim 270 \mu$ m) and thinner than the abactinal and inferomarginal spinelets (Figure 2C, D); tip is rounded, serrated, almost cylindrical in shape, but slightly thicker at the base, covered with small but stout thorns (some might appear serrated), and lacking the longitudinal ridges. Each ambulacral plate bears 2–4, mostly 2, furrow spines, and several numerous actinal spinelets arranged in irregular rows (Figure 2C). Oral plates are prominent abradially and sunken adradially; creating a middle ridge that separates both plates; each oral plate bears 5 oral spines that resemble the actinal spinelets, but somewhat curved, arranged in two groups of 2 proximal and 3 distal; and 3 (sometimes 4) suboral spines arranged 1 (sometimes 2) proximal, 1 central and 1 distal (Figure 2C). Heart-shaped actinal membrane covers the proximal part of each interradius; gonads and odontophores are visible through this membrane; lacking spicules (Figures 1B–D & 2B, C).

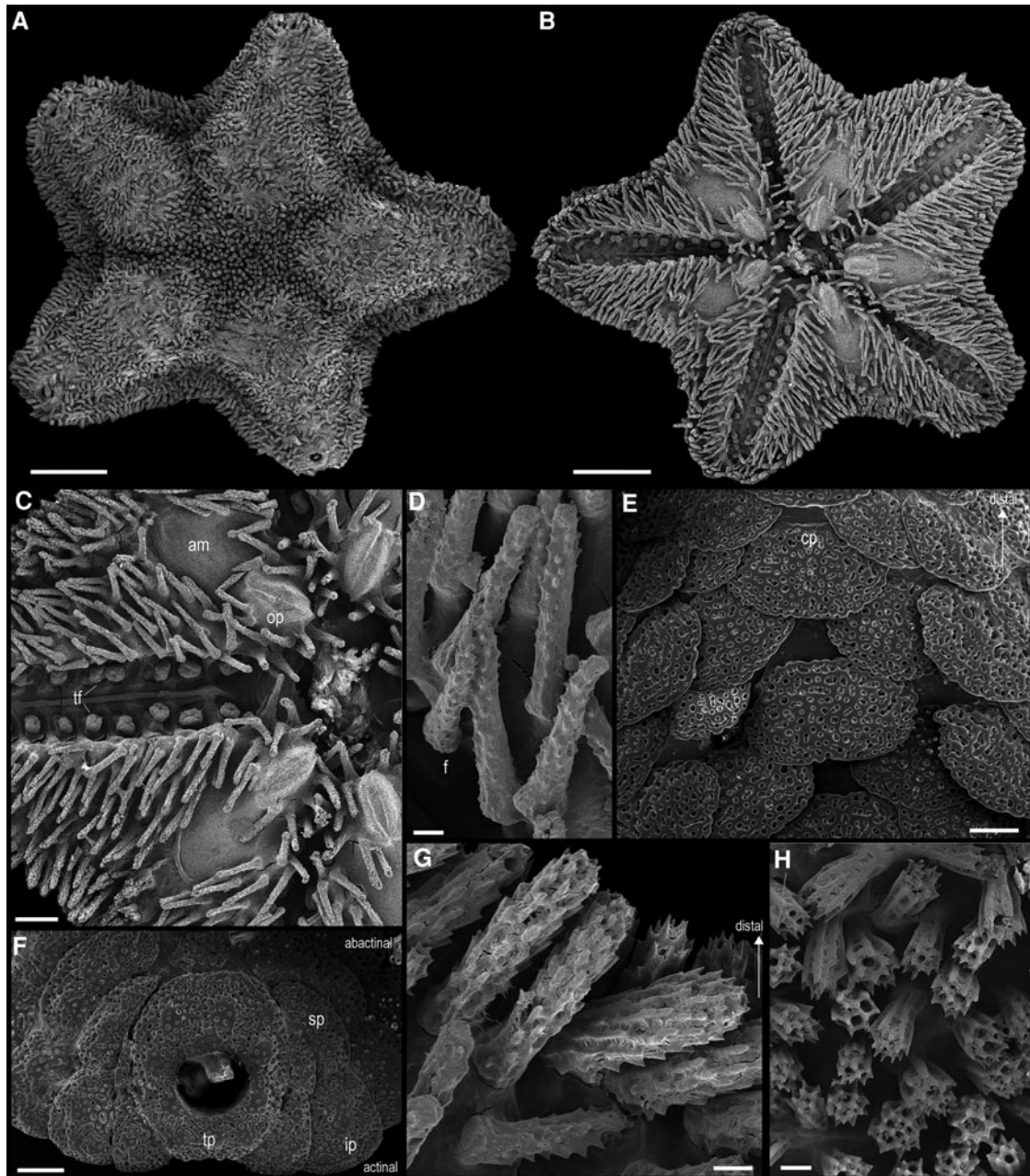


Fig. 2. Scanning electron microscope images of *Crinitostella laguardai* gen. nov., sp. nov. Paratype (ICML-UNAM 18416): abactinal surface (A); actinal surface (B); detail of actinal surface (C); actinal spinelets (D); detail of abactinal surface of the arm (E); terminal plate with pore (F); actinal inferomarginal spinelets (G); abactinal spinelets (H). Scale bars: A, B, 1 mm; C, 250 μ m; D, G, H, 40 μ m; E, F, 100 μ m. am, actinal membrane; op, oral plate; f, furrow; cp, carinal plate; tp, terminal plate; sp, superomarginal plate; ip, inferomarginal plate; tf, tube feet.

Colour

Both *in vivo* and preserved specimens are uniformly white, with abactinal plates of glassy appearance.

Habitat, Distribution and Biology

This species is only known from off Tabasco, Gulf of Mexico, Mexico (19°16.272'N 93°06.69'W to 19°16.045'N 93°04.613'W), from 418–427 m deep. The 12 specimens were found together in a sunken log that was recovered in a trawl. They range in sizes (R) from 2.7–3.9 mm, but gonads are visible through the actinal membrane in all of them, suggesting these to be sexually mature adults.

Phylogenetic analyses

The only sequence of a caymanostellid available on public databases is for the 16S gene of *Caymanostella* sp. (GenBank:

DQ297082). This sequence is 21.6% divergent (K2P distance) from our 16S sequence of *Crinitostella laguardai* gen. nov., sp. nov. The topologies recovered by both BI and ML analyses differed slightly, but both recovered *Caymanostella* sp. and *Crinitostella laguardai* gen. nov., sp. nov. in a well-supported clade (Figure 3). However, the caymanostellids were not recovered within the order Velatida, but rather with a group including the Valvatida, Paxillosida, Notomyotida, and Spinulosida.

Discussion

Crinitostella laguardai gen. nov., sp. nov. represents the first caymanostellid reported for the Gulf of Mexico. This remarkable species was collected from a single site, with all specimens recovered from the same piece of sunken wood. So far, this new species also represents the shallowest bathymetric record, from currently described species, for the family. However, a specimen of an

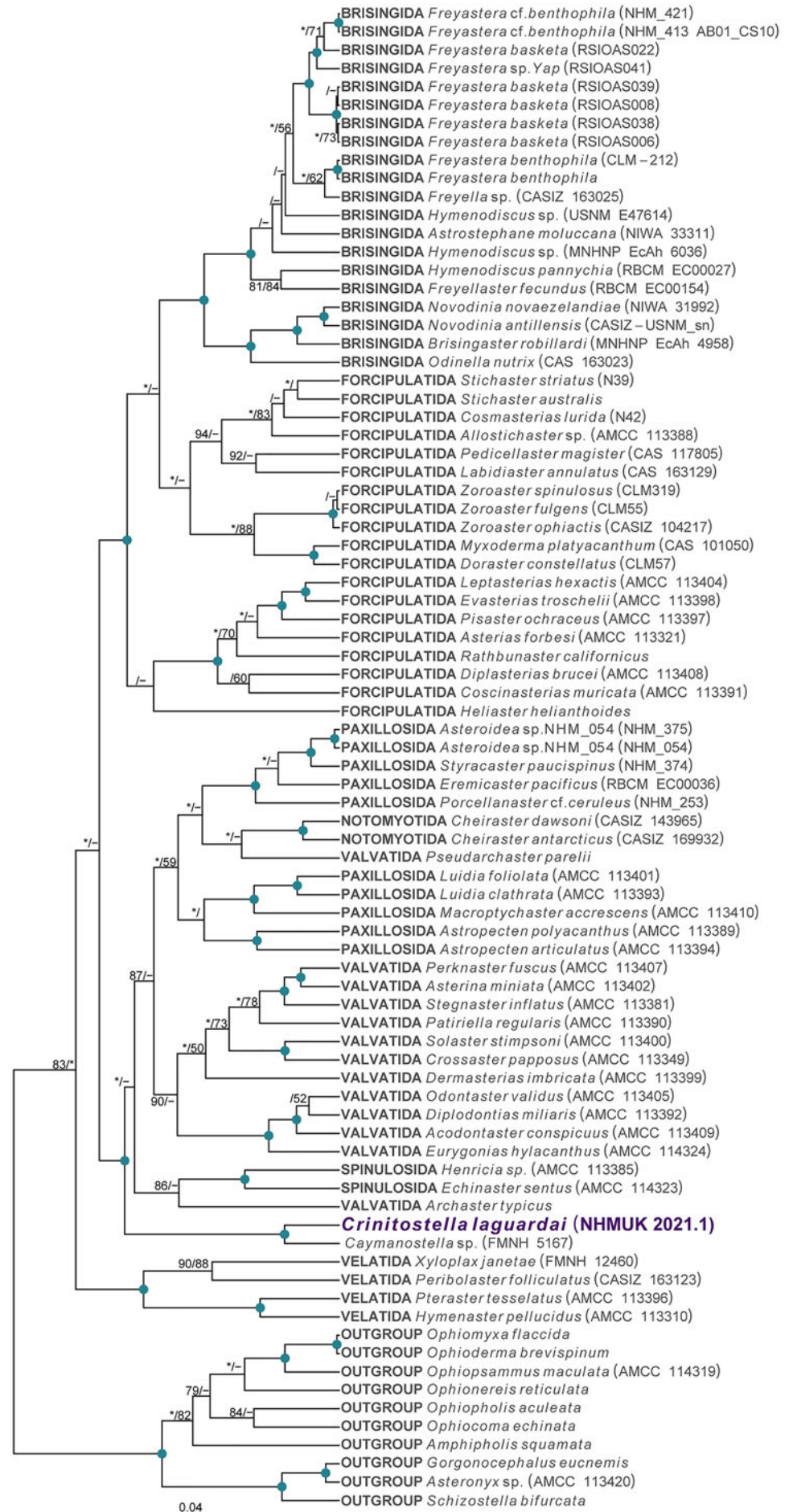


Fig. 3. Rooted Bayesian phylogeny for the Asterozoa. Concatenated (12S, 16S, 18S, 28S, COI and H3) BEAST median consensus tree with posterior probability (PP) and bootstrap (BS) values indicated for each node. Only values of PP > 0.70 and BS > 50 are shown, with values of PP > 0.95 and BS > 90 indicated as a blue circle. Nodes not recovered on the RAxML tree are indicated with -. The specimen for which sequences were generated in this study is highlighted in violet text.

undescribed species of *Caymanostella* was collected at 414–456 m deep in the Solomon Islands (Byrne & O'Hara, 2017).

The family Caymanostellidae displays affinities with several groups, such as Asterinidae and Korethraasteridae, making it difficult to infer its phylogenetic position evidenced by the myriad of contrasting phylogenetic hypotheses proposed (e.g. Blake, 1987; Rowe *et al.*, 1988; Rowe, 1989). Previous molecular analyses recovered the family Caymanostellidae in different phylogenetic positions (Janies *et al.*, 2011). A more recent study, based on phylogenomic data, provided insight into the phylogenetic relationships of the orders within Asterozoa (Linchangco *et al.*, 2017). Unfortunately, no representatives of Caymanostellidae were included and hence their phylogenetic position remains untested by robust phylogenomic methods. In an attempt to shed some light into this matter, we used mitochondrial and nuclear DNA and combined it with the data presented in Janies *et al.* (2011), constraining orders as recovered in Linchangco *et al.* (2017). Our analyses confidently recovered Caymanostellidae outside the Velatida, and in a clade along Paxillosida, Notomyotida, Valvatida and Spinulosida (Figure 4). This result is concordant with Mah & Blake (2012), where the family Caymanostellidae was not retained within Velatida, but instead recovered as part of a valvatacean polytomy. However, further studies with an increased sampling taxon and targeting a large number of loci are required to clarify the phylogenetic relationships of valvataceans.

Supplementary material. The supplementary material for this article can be found at <https://doi.org/10.1017/S0025315421000448>.

Acknowledgements. We are grateful to Adolfo Gracia (ICML, UNAM), chief scientist, to the staff and crew members of RV 'Justo Sierra' during COBERPES 5 in May 2013, as well as scientists on board, especially Andrea Caballero, Julio Arriaga and Mauricio Valdés (ICML, UNAM) for recovering the specimens from the sunken log. We also acknowledge the support of the staff from the Laboratorio de Ecología Pesquera de Crustáceos (ICML, UNAM) for their technical support during the oceanographic campaign. We thank Melanie Mackenzie (MV) and Toshihiko Fujita (NSMT) for access to scientific collections, and Claire Griffin (NHM) for support with sequencing. We also thank Andrew Cabrinovic and Lauren Hughes (NHM), Alicia Durán and Ma. Esther Diupotex (ICML, UNAM) for access to scientific collections and for the support provided accessing the material into the different scientific collections. We acknowledge Susana Guzmán Gómez and Berenit Mendoza Garfias (IB, UNAM) for technical assistance with photography. Project IN223109-3 was funded by Proyectos de Investigación e Innovación Tecnológica (PAPIIT) UNAM. We are also grateful to two anonymous reviewers for their comments that greatly improved this manuscript.

Author contributions.

CMCR and GBC carried out the morphological analyses; GBC performed the phylogenetic analyses. All authors contributed to writing the manuscript.

References

- Aziz A and Jangoux M** (1984) Description de quatre nouvelles espèces d'asteroïdes profonds (Echinodermata) de la région Indo-Malaise. *Indo-Malayan Zoology* **2**, 187–194.
- Belyaev GM** (1974) A new family of abyssal starfishes. *Zoologicheskii Zhurnal* **53**, 1502–1508.
- Blake DB** (1987) A classification and phylogeny of post-Palaeozoic sea stars (Asterozoa: Echinodermata). *Journal of Natural History* **21**, 481–528.
- Bouckaert R, Heled J, Kuhnert D, Vaughan T, Wu CH, Xie D, Suchard MA, Rambaut A and Drummond AJ** (2014) BEAST 2: a software platform for Bayesian evolutionary analysis. *PLoS Computational Biology* **10**, e1003537.
- Byrne M and O'Hara TD** (2017) *Australian Echinoderms: Biology, Ecology and Evolution*. Clayton: CSIRO Publishing.
- Castresana J** (2000) Selection of conserved blocks from multiple alignments for their use in phylogenetic analysis. *Molecular Biology and Evolution* **17**, 540–552.
- Colgan DJ, Ponder WF, Beacham E and Macaranas JM** (2003) Gastropod phylogeny based on six segments from four genes representing coding or non-coding and mitochondrial or nuclear DNA. *Molluscan Research* **23**, 123–148.
- Janies DA, Voight JR and Daly M** (2011) Echinoderm phylogeny including *Xyloplax*, a progenetic asteroid. *Systematic Biology* **60**, 420–438.
- Katoh K, Rozewicki J and Yamada KD** (2019) MAFFT Online service: multiple sequence alignment, interactive sequence choice and visualization. *Briefings in Bioinformatics* **20**, 1160–1166.
- Kumar S, Stecher G, Li M, Knyaz C and Tamura K** (2018) MEGA X: Molecular Evolutionary Genetics Analysis across computing platforms. *Molecular Biology and Evolution* **35**, 1547–1549.
- Lanfear R, Frandsen PB, Wright AM, Senfeld T and Calcott B** (2017) PartitionFinder 2: new methods for selecting partitioned models of evolution for molecular and morphological phylogenetic analyses. *Molecular Biology and Evolution* **34**, 772–773.
- Linchangco GV Jr, Foltz DW, Reid R, Williams J, Nodzak C, Kerr AM, Miller AK, Hunter R, Wilson NG, Nielsen WJ, Mah CL, Rouse GW, Wray GA and Janies DA** (2017) The phylogeny of extant starfish (Asterozoa: Echinodermata) including *Xyloplax*, based on comparative transcriptomics. *Molecular Phylogenetics and Evolution* **115**, 161–170.
- Mah CL** (2019) World Asterozoa Database. Caymanostellidae Belyaev, 1974. Accessed through *World Register of Marine Species*. Available at <http://www.marinespecies.org/aphia.php?p=taxdetails&id=177886> (Accessed 27 August 2019).
- Mah CL and Blake DB** (2012) Global diversity and phylogeny of the Asterozoa (Echinodermata). *PLoS ONE* **7**, e35644.
- McKnight DG** (2006) The marine fauna of New Zealand: Echinodermata: Asterozoa (Sea-stars). 3. Orders Velatida, Spinulosida, Forcipulatida, Brisingida with addenda to Paxillosida, Valvatida. *NIWA Biodiversity Memoir* **120**, 1–187.
- Palumbi SR** (1996) Nucleic acid II: the polymerase chain reaction. In Hillis DM, Moritz G and Mable BK (eds), *Molecular Systematics*. Sunderland, MA: Sinauer Associates, pp. 205–247.
- Ramirez JM, Vazquez-Bader AR and Gracia A** (2019) Ichthyofaunal list of the continental slope of the southern Gulf of Mexico. *Zookeys* **846**, 117–132.
- Rowe FWE** (1989) A review of the family Caymanostellidae (Echinodermata: Asterozoa) with the description of a new species of *Caymanostella* Belyaev and a new genus. *Proceedings of the Linnean Society of New South Wales* **111**, 293–307.
- Rowe FWE, Baker AN and Clark HES** (1988) The morphology, development and taxonomic status of *Xyloplax* Baker, Rowe and Clark (1986) (Echinodermata: Concentricycloidea), with the description of a new species. *Proceedings of the Royal Society of London. Series B. Biological Sciences* **233**, 431–459.
- Smith AB** (1988) To group or not to group: the taxonomic position of *Xyloplax*. In Burke RD, Mladenov PV, Lambert P and Parsley RL (eds), *Echinoderm Biology: Proceedings of the Sixth International Echinoderm Conference*, Victoria, Canada, 23–27 August 1987. Rotterdam: A.A. Balkema.
- Stamatakis A** (2006) RAxML-VI-HPC: maximum likelihood-based phylogenetic analyses with thousands of taxa and mixed models. *Bioinformatics* **22**, 2688–2690.